AGU PUBLICATIONS

Geophysical Research Letters

RESEARCH LETTER

10.1002/2014GL060369

Key Points:
- We present a time series of sea ice thickness in Fram Strait from in situ data
- Fram Strait sea ice thickness has decreased by over 50% in 2003–2012
- The thinning independent from the source region indicates Arctic-wide decline

Supporting Information:
- Readme
- Figure S1
- Figure S2
- Figure S3

Correspondence to:
A. H. H. Renner,
angelika.renner@imr.no

Citation:
Renner, A. H. H., S. Gerland, C. Haas, G. Spreen, J. F. Beckers, E. Hansen, M. Nicolaus, and H. Goodwin (2014), Evidence of Arctic sea ice thinning from direct observations, *Geophys. Res. Lett.*, *41*, doi:10.1002/2014GL060369.

Received 29 APR 2014
Accepted 19 JUN 2014
Accepted article online 24 JUN 2014

Evidence of Arctic sea ice thinning from direct observations

Angelika H. H. Renner[1,2], Sebastian Gerland[1], Christian Haas[3], Gunnar Spreen[1], Justin F. Beckers[4], Edmond Hansen[1,5], Marcel Nicolaus[6], and Harvey Goodwin[1]

[1]Norwegian Polar Institute, Fram Centre, Tromsø, Norway, [2]Now at Institute of Marine Research, Tromsø, Norway, [3]Department of Earth and Space Science and Engineering, York University, Toronto, Ontario, Canada, [4]Department of Earth and Atmospheric Sciences, University of Alberta, Edmonton, Alberta, Canada, [5]Now at Multiconsult, Tromsø, Norway, [6]Alfred Wegener Institute, Helmholtz Centre for Polar and Marine Research, Bremerhaven, Germany

Abstract The Arctic sea ice cover is rapidly shrinking, but a direct, longer-term assessment of the ice thinning remains challenging. A new time series constructed from in situ measurements of sea ice thickness at the end of the melt season in Fram Strait shows a thinning by over 50% during 2003–2012. The modal and mean ice thickness along 79°N decreased at a rate of 0.3 and 0.2 m yr^{-1}, respectively, with long-term averages of 2.5 and 3 m. Airborne observations reveal an east-west thickness gradient across the strait in spring but not in summer due to advection from more different source regions. There is no clear relationship between interannual ice thickness variability and the source regions of the ice. The observed thinning is therefore likely a result of Arctic-wide reduction in ice thickness with a potential shift in exported ice types playing a minor role.

1. Introduction

Recent changes in the Arctic sea ice cover are most obvious in the drastic decline in the summer ice extent [e.g., *Parkinson and Comiso*, 2013]. Other indicators include a decrease of multiyear ice [*Maslanik et al.*, 2011; *Comiso*, 2012], an increase in drift speed and deformation rate [*Rampal et al.*, 2009; *Spreen et al.*, 2011], and a basin-wide thinning of the ice cover [*Kwok et al.*, 2009] and ice volume loss [*Laxon et al.*, 2013]. However, interannual variability is large [e.g., *Kwok et al.*, 2013] and long time series especially of sea ice thickness are scarce. *Hansen et al.* [2013] present ice draft observations over 22 years (1990–2011) from moored instruments in Fram Strait showing a decrease in thickness and amounts of old level ice. However, their data set is geographically limited to one point at 79°N, 5°W. *Haas et al.* [2008] and *Haas* [2013] observe a similar decline in ice thickness in the Transpolar Drift using data from different campaigns in 1991–2007 and 1975–2012, respectively. *Perovich et al.* [2014] did not find a definitive trend in their observations, especially of surface and bottom melt from Ice Mass Balance buoys deployed near the North Pole between 2000 and 2013.

Currently, approximately 15% of the total ice volume are exported annually from the central Arctic. The majority of this export happens through Fram Strait, the passage between Greenland and Svalbard [*Kwok*, 2009; *Spreen et al.*, 2009]. The sea ice in Fram Strait can originate from different regions of the Arctic Ocean [see, e.g., *Pfirman et al.*, 2004; *Kwok*, 2009; *Hansen et al.*, 2013] and has thus varying age and degree of deformation. Therefore, changes in the Fram Strait ice cover reflect and integrate processes in the central Arctic making this a key region for observations.

While *Hansen et al.* [2013] used a time series of sea ice draft from moorings at a fixed location (79°N, 5°W), we now present a 10 year time series of in situ and airborne observations of ice thickness collected annually along 79°N between Svalbard and Greenland, spatially extending *Hansen et al.*'s [2013] study. In particular, the airborne measurements cover most of the width of the ice tongue in Fram Strait, providing information about the spatial thickness distribution. We investigate the connection between the observed ice thickness variability and source regions and other ice properties.

2. Methods and Data Sets

In this study, we analyze sea ice thickness measurements obtained using ground-based and airborne electromagnetic (EM) instruments during multiple cruises to the Fram Strait from 2003 to 2012 (see Table 1 and Figure S1 in the supporting information). All EM systems make use of the principles of electromagnetic induction at the seawater/sea ice interface. On the ground, we used a Geonics EM31 portable instrument placed on top of the snow or weathered ice surface and with a footprint size of approximately 3–4 m

Table 1. Overview of Ship Campaigns and Basic Ice and Snow Thickness Statistics for Each Method[a]

Campaign	Dates	Ship	Number of Observations EM31/Snow/HEM	Mode (m) EM31/Snow/HEM	Mean (m) EM31/Snow/HEM
FS2003	7–27 Sep 2003	R/V *Lance*	207/47/–	4.2/0.02/–	4.0 ± 1.3/0.01 ± 0.01/–
FS2004	31 Aug to 19 Sep 2004	R/V *Lance*	206/205/–	3.2/0.02/–	3.5 ± 0.9/0.04 ± 0.03/–
F2005	18 May to 4 Jun 2005	K/V *Svalbard* and R/V *Lance*	918/936/358333	2.0/0.2/2.8	2.5 ± 1.1/0.32 ± 0.22/2.6 ± 1.7
FS2005	29 Aug to 17 Sep 2005	R/V *Lance*	163/163/–	3.4/0.04/–	3.6 ± 1.0/0.06 ± 0.03/–
FS2006	31 Aug to 16 Sep 2006	R/V *Lance*	105/105/–	2.4/0.1/–	3.0 ± 0.6/0.18 ± 0.11/–
F2007	10–30 Apr 2007	K/V *Svalbard*	883/882/–	2.1/0.3/–	2.5 ± 0.9/0.47 ± 0.24/–
FS2007	10–30 Sep 2007	R/V *Lance*	339/322/–	1.6/0.18/–	2.8 ± 1.1/0.20 ± 0.08/–
F2008	16 Apr to 1 Jun 2008	K/V *Svalbard*	2613/1057/302043	3/0.2/2.2	3.2 ± 1.1/0.39 ± 0.22/2.7 ± 1.6
FS2008	30 Aug to 19 Sep 2008	R/V *Lance*	684/680/–	1.8/0.04/–	2.5 ± 1.3/0.05 ± 0.03/–
FS2009	30 Aug to 24 Sep 2009	R/V *Lance*	671/772/–	1.8/0.04/–	2.7 ± 1.7/0.06 ± 0.04/–
FS2010	3–18 Sep 2010	R/V *Lance*	896/753/53397	1.8/0.1/1.2	2.3 ± 1.2/0.11 ± 0.04/1.4 ± 0.8
FS2011	22 Aug to 15 Sep 2011	RV *Lance*	2140/753/160718	1.4/0.04/1.0	2.4 ± 1.0/0.08 ± 0.06/1.3 ± 1.3
FS2012	19 Aug to 5 Sep 2012	RV *Lance*	2341/2532/138160	1.6/0.06/1.4	2.7 ± 1.3/0.08 ± 0.05/1.1 ± 1.1

[a]Number of observations, mode, and mean ± standard deviation are given for each measurement method used in a campaign (EM31 = ground-based ice thickness measurements; snow = snow thickness measurements; HEM = airborne ice thickness measurements; "–" = no measurements were done using this method).

[see, e.g., *Haas et al.*, 1997]. The data were calibrated using drill hole measurements and processed following *Haas et al.* [1997]. During 2003 to 2008, readings were taken every 5 m. From 2009, values were logged automatically every 2 s while the EM31 was pulled on a sled across the ice. For these data sets, we use simultaneous GPS measurements to resample observations at 4 m spacing to avoid spatially overlapping measurements. The airborne system (the so-called EM-bird, *Haas et al.* [2009]) is towed below a helicopter and provides measurements with a footprint of approximately 50 m and an accuracy of 0.1 m over level ice. Both EM systems record total snow and ice thickness, in the following referred to as ice thickness. Snow depth was measured every 5 m along the EM31 transects using a metal probe.

The annual August/September cruises onboard R/V *Lance* led by the Norwegian Polar Institute (NPI) cover the width of Fram Strait along approximately 79°N with occasional additional transects farther north and off the coast of East Greenland. In this study, we only include data collected over drift ice, excluding measurements obtained over iceberg-fast sea ice near the East Greenland coast. For each cruise, we calculate probability density functions (pdf) of ice and snow thickness from all measurements during a cruise, and derive the mean and modal thickness from these pdfs. To assess the zonal variability along 79°N, we bin the EM-bird measurements in 0.1° longitudinal bins and calculate pdfs, mean, and mode in those bins.

Back trajectories of sea ice parcels (i.e., groups of floes) are calculated using a combination of observations and model simulations. The primary data set used are satellite sea ice drift observations obtained from merged Special Sensor Microwave Imager and Quick Scatterometer data [*Girard-Ardhuin et al.*, 2008; *Girard-Ardhuin and Ezraty*, 2012]. Due to the wetting of the snow and ice surface during summer, reliable satellite ice drift estimates are not obtained between June and August (for some years also not in May and September). To bridge that summer gap, ice drift estimates from a coupled ocean-sea ice model with atmospheric forcing from the JRA-25 reanalysis [*Onogi et al.*, 2007] and horizontal grid spacing of 4.5 km are used [*Nguyen et al.*, 2011, 2012]. Back trajectories are calculated for 2 years starting from 15 different positions between 15°W and 1°W at 79°N. For the late summer campaigns, the back trajectory calculation is started on 15 August. For the spring campaigns in 2005, 2007, and 2008, the back trajectories are started on 1 April. Ice parcels are considered lost when they encounter ice concentrations below 15% for four consecutive days or approach land. Tracking over 2 years gives enough time to allow for a clear distinction of the source regions.

3. Sea Ice Thickness

During 2003–2011, the overall mean and modal ice thickness of drift ice in Fram Strait measured by EM31 in late summer at the end of the melt season is 3.0 and 2.5 m, respectively. At the time of the measurements in late summer, the snow depth is minimal (Figure 1a and Table 1) as all old snow had melted and the only snow that was observed was new snow that fell during or just prior to the campaigns. The time series of EM31-derived mean and modal ice thickness (Figure 1a) shows a statistically significant decrease of

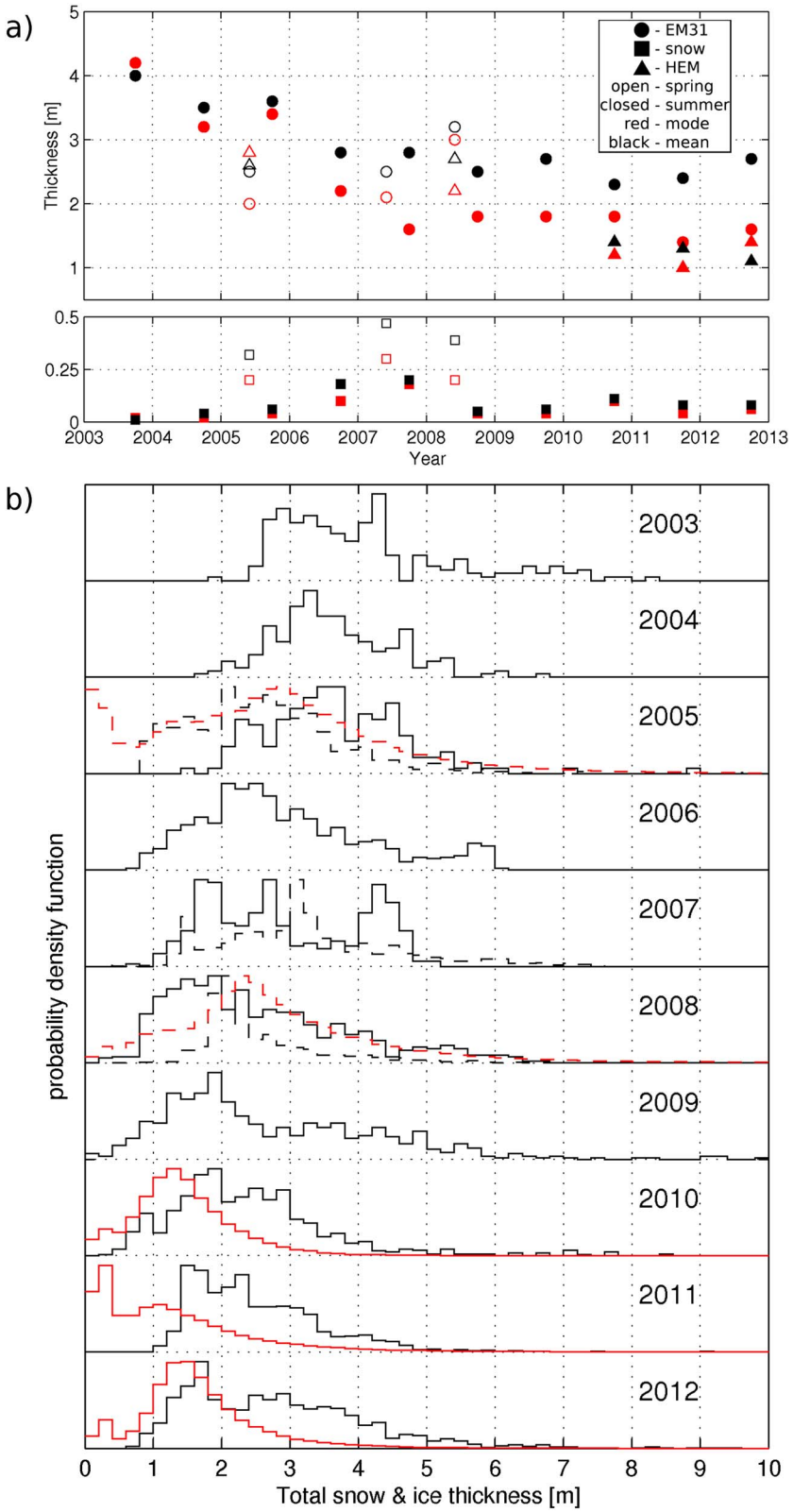

Figure 1. (a) Mean (black) and mode (red) of snow (squares) and total ice and snow thickness distributions (circles = EM31 surveys; triangles = EM-bird surveys). Solid symbols show results from the August/September campaigns, open symbols the spring results. Note the scaling on the split *y* axis. (b) Ice thickness distributions from EM31 (black lines) and HEM measurements (red lines) from 2003 (top) to 2012 (bottom). Solid lines show measurements in late summer, dashed lines measurements in spring.

0.2 and 0.3 m yr^{-1}, respectively, over the entire period ($p > 0.99$ using Student's t test). However, the shape of the time series suggest a strong decrease during the first 4–5 years followed by very little change in the next 5–6 years. Piecewise linear fitting [*Tome and Miranda*, 2004] of two fits per time series confirm this. The resulting trend changing points for modal and mean thickness are in 2007 and 2008, respectively. The trends are −0.3 m yr^{-1} in 2003–2008 for the mean, and −0.6 m yr^{-1} in 2003–2007 for the mode, about twice as much as for the entire time series. For the periods after 2007/2008, no significant trend in ice thickness can be observed. The three spring campaigns (Figure 1a, open symbols) show high interannual variability, partially due to deep snow.

EM31 transects are spatially limited due to logistical and safety reasons. This restricts the number of independent observations and can lead to pdfs that are not as smooth as, e.g., EM-bird-derived pdfs. Also, very thin ice cannot be surveyed for safety reasons resulting in a bias toward thicker ice. A comparison of EM31 mean and modal ice thicknesses with observations from upward looking sonars (ULS) moored to the seafloor in Fram Strait [*Hansen et al.*, 2013] yields very close agreement both in absolute numbers and trend despite the very different methods and biases in the data sets (Figure S2 in the supporting information). Multiple modes exist in late summer 2006, 2007, and 2011 (Figure 1b). Using the second, thicker ice mode for these years in the time series shown in Figure 1a does not change the trend in the modal ice thickness (−0.3 m yr^{-1}). Percentiles are less sensitive to the shape of the distributions. We therefore also calculated percentiles at various thresholds (10, 25, 50, 75, and 90%) for the late summer pdfs. The time series show a consistent decrease at all levels (Figure 3a in the supporting information) similar in shape to the development of the mode and the mean. EM31 transect lengths vary from floe to floe. It can therefore be argued that statistics such as mean and modal thickness should be calculated per floe before deriving a cruise average. Using this approach does not significantly change our results (not shown).

Since footprint size and spatial coverage of EM31 and EM-bird measurements are orders of magnitude different (3–4 m versus 50 m for the footprint and 1 km versus 100 km for the spatial coverage), direct comparison of the results of the two methods is difficult. Except for spring 2005, the EM-bird surveys give lower ice thicknesses than the EM31 transects. This can largely be explained by the effect of open water under the EM-bird. While the EM31 transects exclude any open water, the EM-bird ice thickness at any one point is the average over both ice and open water fraction within the footprint of the EM-bird. In dynamic regions such as Fram Strait, especially in late summer, ice floes can be relatively small (< 100 m) and the open water fraction high (> 25%). For late summer 2010, we can estimate an adjusted ice thickness distribution using simultaneous EM-bird measurements and aerial photographs [*Renner et al.*, 2013] by dividing ice thickness by ice concentration, thereby compensating for measurements near floe edges. The adjusted mean and modal thicknesses are 1.8 and 1.4 m, respectively, slightly higher than the original values (1.4 and 1.2 m) but still lower than the EM31 observations of 2.3 and 1.8 m. Besides open water, the EM31 measurements also underestimate the amount of thin ice since very thin ice and brash ice cannot be measured due to safety reasons. The thin ice classes are therefore absent in the EM31-derived pdfs. They are, however, present in the EM-bird data, and observations from the helicopter and aerial photographs confirm a large amount of brash ice during the late summer campaigns in 2010–2012. When combined, the open water and thin ice bias in the EM31 data together with the aforementioned bias due to considerations around floe choice are likely responsible for the differences in mean and mode between EM31 and EM-bird. However, the biases in the EM31 data are assumed consistent throughout the time series presented here.

The challenges encountered when trying to compare measurements using the same general technique in the same general region are amplified when using observations (a) with the same technique in a different region (even if "only" upstream [e.g., *Haas et al.*, 2008]), (b) in the same region but with different techniques [e.g., *Hansen et al.*, 2013], or worst of all, (c) in different regions and with different techniques (e.g., buoys [*Perovich et al.*, 2014], airborne or satellite remote sensing [*Kwok et al.*, 2009; *Laxon et al.*, 2013; *Richter-Menge and Farrell*, 2013], or submarine data [e.g., *Kwok and Rothrock*, 2009]). A dedicated study into correct methods of combining different data sets is needed and care has to be taken when using data from different sources, especially for quantitative comparisons.

When looking at the spatial distribution of ice thickness along 79°N (Figure 2), we find in spring an east-west gradient in the EM-bird data with the thickest ice in the western part of the transect. In spring 2008, the section between approximately 12°W and 9°W is strongly influenced by the Northeast Water Polynya which is a recurring feature in the northwestern Fram Strait [e.g., *Bourke et al.*, 1987]. Using only observations

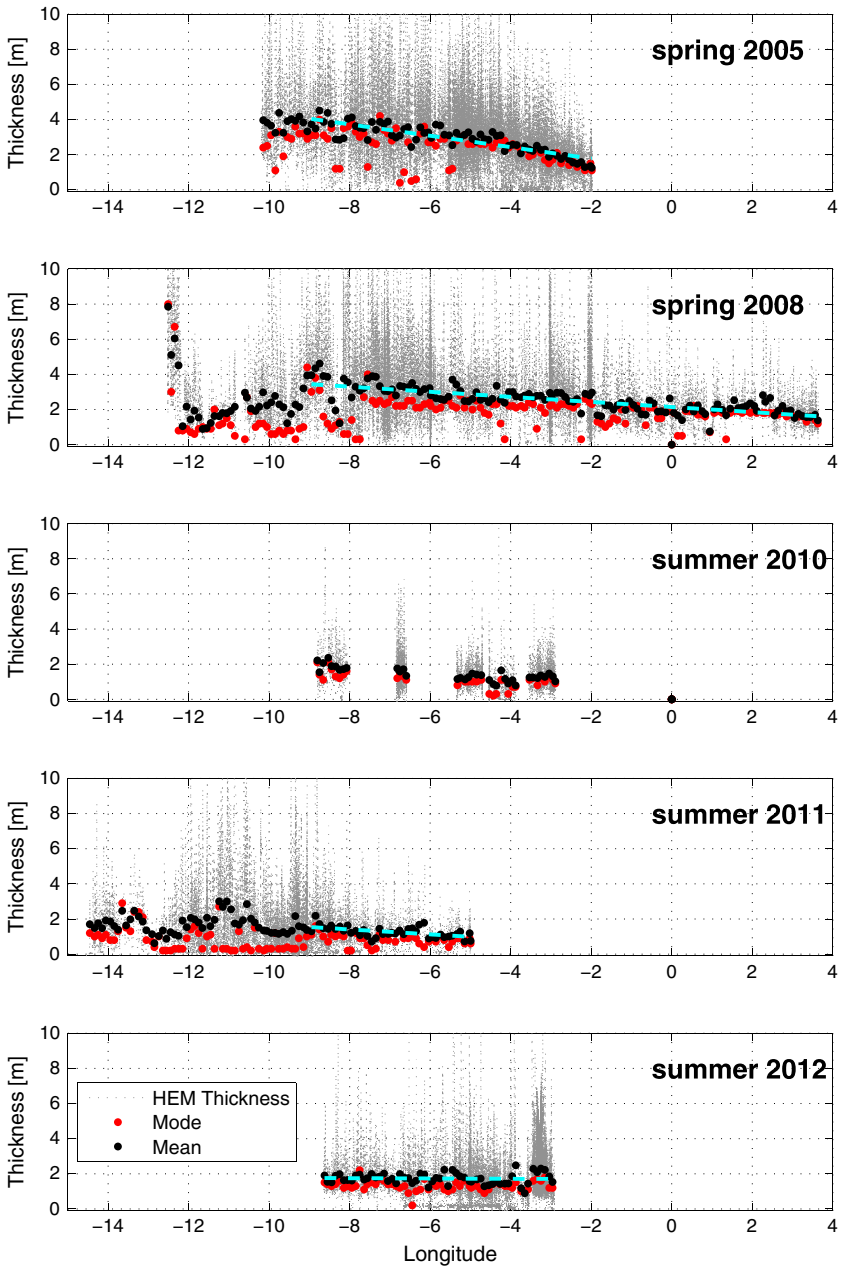

Figure 2. Sea ice thickness versus longitude in Fram Strait. The grey lines mark all measurements; the red and black dots show the mode and the mean of the ice thickness distribution, respectively, in each 0.1° longitude bin. The *y* axes are capped at 10 m. Light blue lines indicate the gradient in mean ice thickness across Fram Strait between −9°W and the ice edge.

east of 9°W, the gradient across the strait is −0.3 m per degree longitude in 2005 and −0.1 m per degree in 2008. This roughly agrees with the ULS ice thickness gradient of −0.23 m per degree between 7°W and 3°W reported by *Hansen et al.* [2013]. However, the gradient is weaker in the late summer observations in 2011 and not present in August/September 2012. In 2010, the spatial coverage is not sufficient to assess such a pattern.

4. Source Region and Other Parameters

While sea ice in Fram Strait is strongly influenced by processes occurring in the Arctic Basin, relationships between ice conditions in the strait and basin wide are not straightforward and easy to determine. The

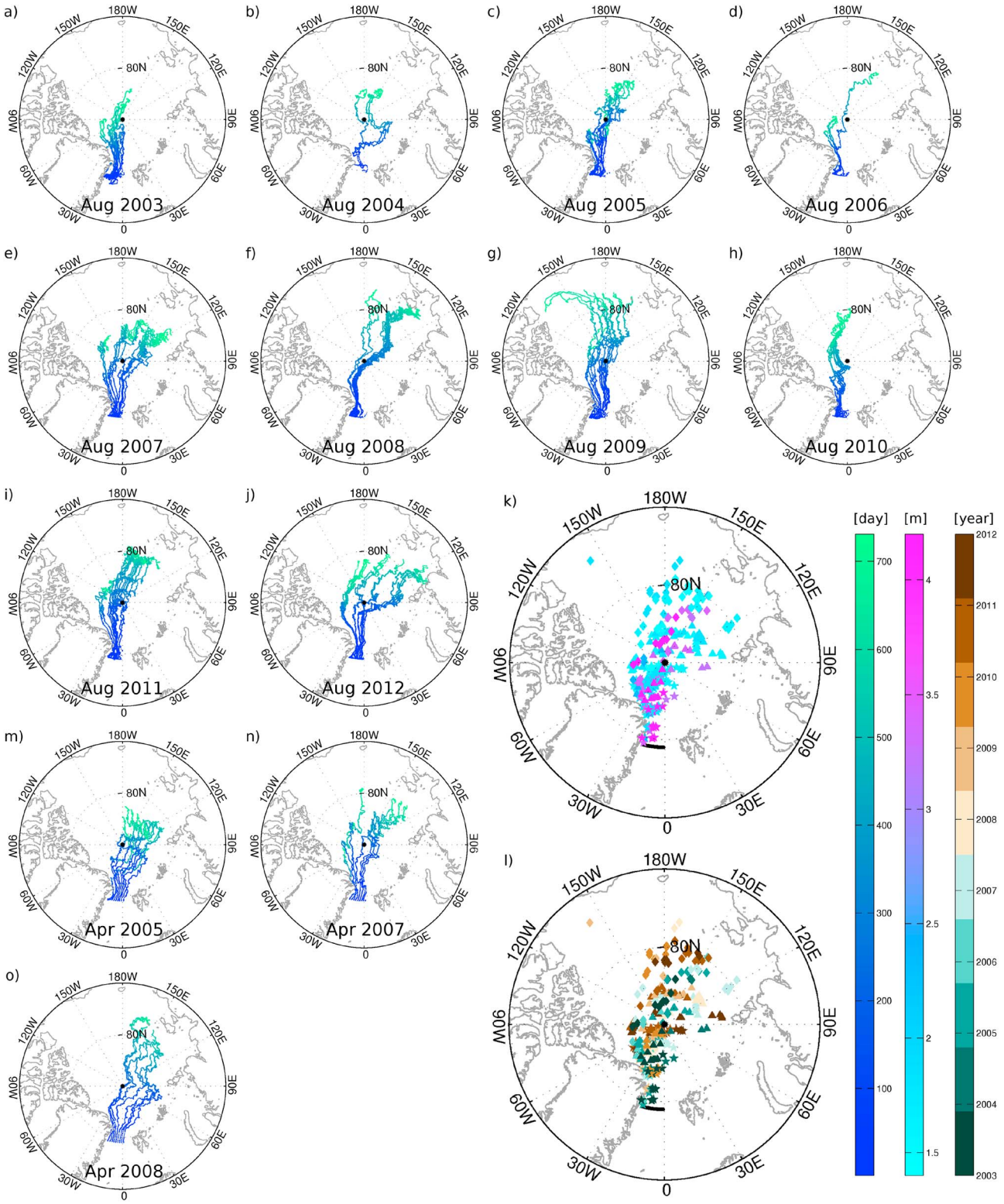

Figure 3. (a–j) Backward drift trajectories for (Figure 3a) 2003 through to (Figure 3j) 2012 color coded by the number of days until crossing 79°N in Fram Strait on 1 August. (k and l) The positions of the trajectories at 180 (stars), 360 (triangles), and 720 days (diamonds) prior to reaching 79° color coded by modal ice thickness and year of measurements, respectively. Black dots indicate the start points of the backtracking. Trajectories for (m) 2005, (n) 2007, and (o) 2008 color coded as in Figures 3a–3j but started on 15 April. All trajectories stop after 2 years (if the particle was not lost before).

summer ice edge and ice concentrations in Fram Strait are largely determined by dynamic processes. As expected, we did not find any connections between observed ice thickness, width of the Fram Strait ice tongue at 79°N, and the Arctic-wide sea ice extent. *Hansen et al.* [2013] suggest a link between thickness and ice age as derived by *Maslanik et al.* [2011]; however, using their data, we do not find such a relationship for our late summer time series.

Backward trajectories of the drift of sea ice parcels are, similar to the ice thickness in an outflow region such as Fram Strait, an integrative measure as they are indicators of what processes will have affected the ice on the way to Fram Strait. Figures 3a–3j show all trajectories calculated for 2003–2012 with day 0 being 15 August and calculated for up to 2 years backward. Variability between years is large, and there is no temporal trend for source regions (Figure 3l). However, both distance traveled along the tracks and distance from the start point are increasing over the 10 year period. Furthermore, ice thickness and distance (both along track and from start point) are anticorrelated, i.e., thin ice traveled farther. We did not find a relationship between source region and ice thickness (Figure 3k).

Throughout the study period, the tracks started in late summer traveled on a narrow band through Fram Strait down to 79°N. Trajectories started in spring (Figures 3m–3o), however, spread out early on and cover a much wider area for the entire 2 years. This suggests that in summer, the ice floes are subject to more dynamic deformation across the width of the strait whereas in spring, a denser ice cover reduces the impact of deformation and instead preserves the ice characteristics from further upstream. Tracks started in spring 2005 (Figure 3m) were considerably shorter than in 2008 (Figure 3o), when within the 2 years, the tracks nearly reached the Siberian coast. The shorter trajectories in 2005 suggest more multiyear ice in the western part of the transect, which explains the larger observed zonal gradient in ice thickness than in 2008.

The increase in travel distance is in agreement with a more mobile ice pack with increasing drift speeds as observed by *Rampal et al.* [2009] and *Spreen et al.* [2011]. Especially the speed up of the Transpolar Drift stream as shown in *Kwok et al.* [2013] is in agreement with the longer trajectories in recent years. *Perovich et al.* [2014] find a positive correlation between southward distance traveled by their buoys and bottom melt, while *Kwok et al.* [2013] also observe a clear anticorrelation between the decrease in multiyear ice fraction and increase in drift speed. As multiyear ice can serve as a proxy for thick ice, this is also in agreement with the anticorrelation between ice thickness decrease and drift trajectory length, i.e., ice speed, increase in this study. More importantly, the missing connection between thickness and source region suggests that the thinning in Fram Strait, while certainly influenced by a potential shift in exported ice types with different ice thickness, can mainly be attributed to the reported Arctic-wide thinning [*Kwok et al.*, 2009; *Laxon et al.*, 2013], which dominates the sea ice thickness variability in Fram Strait.

5. Summary and Conclusions

We presented a 10 year time series of in situ sea ice thickness data from Fram Strait, supplemented with airborne measurements. Over the period 2003–2012, late summer mean and modal ice thickness decreased by over 50%, confirming and extending the trends found by *Hansen et al.* [2013] using a different method. The strongest decrease in both mean and modal thickness occurred between 2003 and 2008. During the same time period, the strong Arctic-wide decrease in ice thickness was observed in the Ice, Cloud, and Land Elevation Satellite (ICESat) record [*Kwok et al.*, 2009]. Thereafter, the observed thickness stabilizes on a low level. *Richter-Menge and Farrell* [2013] observed a similar development for the multiyear ice north of Greenland. Backtracking trajectories showed no trend in source region or relationship to ice thickness consistent with the observed basin-wide thinning of the Arctic ice cover. An increase in travel distance agrees with observations of higher drift speeds. The spatial coverage in our data adds information about the ice thickness distribution across Fram Strait to the single point ULS time series by *Hansen et al.* [2013]. In spring 2005 and 2008, a clear gradient in ice thickness across Fram Strait is visible and likely due to a widespread of source regions whereas a narrower transport corridor during summer leads to the absence of such a gradient at the end of the melt season.

The time series presented here was put together from a large number of observations each covering only a small area. The comparison between ground-based and airborne EM demonstrated the problems around footprint sizes, sampling biases, and influence of ice conditions in a challenging region such as Fram Strait in summer with small ice floes, lots of brash ice, and a high open water fraction. These problems increase

when trying to compare results to measurements using different methods (e.g., laser or radar altimetry) and platforms such as planes (e.g., from the IceBridge campaigns [*Kurtz et al.*, 2012] or satellites such as ICESat or CryoSat-2 [e.g., *Kwok et al.*, 2009; *Laxon et al.*, 2013]). Dedicated studies are needed to find appropriate comparison and upscaling techniques. While in situ measurements offer limited temporal sampling, they are, however, the only direct method to unambiguously measure the ice thickness without any assumptions about densities, snow, etc., or models involved. The data presented here confirm the strong changes observed in the Arctic sea ice cover during the recent decade.

Acknowledgments

We thank the crews and captains of R/V *Lance* and K/V *Svalbard*, the teams of Airlift AS, and the many helpers in the field, in particular M. Bratrein, M.A. Granskog, R. Hall, S.R. Hudson, B. Kuipers, A. Nicolaus, O.M. Olsen, and C.A. Pedersen (all NPI). This study is part of the NPI ICE Centre project "ICE-Fluxes" and NPI's long-term sea ice thickness monitoring. Additional support came from the EU project "Damocles," the Norwegian Research Council IPY-project "IAOOS-Norway," the Norwegian Space Centre and ESA PRODEX project "CryoSat postlaunch validation study for sea ice," and the Fram Centre through the project "Sea Ice in the Arctic Ocean, Technology and Systems of Agreements," subproject "CASPER." The data presented here can be requested from the authors and will soon be available from NPI's data portal.

The Editor thanks two anonymous reviewers for their assistance in evaluating this paper.

References

Bourke, R. H., J. L. Newton, R. G. Paquette, and M. D. Tunnicliffe (1987), Circulation and water masses of the East Greenland shelf, *J. Geophys. Res.*, *92*(C7), 6729–6740.

Comiso, J. C. (2012), Large decadal decline of the Arctic multiyear ice cover, *J. Clim.*, *25*, 1176–1193, doi:10.1175/JCLI-D-11-00113.1.

Girard-Ardhuin, F., and R. Ezraty (2012), Enhanced Arctic sea ice drift estimation merging radiometer and scatterometer data, *IEEE Trans. Geosci. Remote Sens.*, *50*, 2639–2648, doi:10.1109/TGRS.2012.2184124.

Girard-Ardhuin, F., R. Ezraty, D. Croize-Fillon, and J. Piolle (2008), Sea ice drift in the central Arctic combining QuikSCAT and SSM/I sea ice drift data, *Technical manual*, CERSAT/Ifremer, Brest, France.

Haas, C. (2013), Arctic sea ice—Where are we headed?, *Proceedings of the 22nd International Conference on Port and Ocean Engineering under Arctic Conditions,* Espoo, Finland, 9–13 June.

Haas, C., S. Gerland, H. Eicken, and H. Miller (1997), Comparison of sea-ice thickness measurements under summer and winter conditions in the Arctic using a small electromagnetc induction device, *Geophysics*, *62*(3), 749–757.

Haas, C., A. Pfaffling, S. Hendricks, L. Rabenstein, J.-L. Etienne, and I. Rigor (2008), Reduced ice thickness in arctic transpolar drift favors rapid ice retreat, *Geophys. Res. Lett.*, *35*, L17501, doi:10.1029/2008GL034457.

Haas, C., J. Lobach, S. Hendricks, L. Rabenstein, and A. Pfaffling (2009), Helicopter-borne measurements of sea ice thickness, using a small and lightweight, digital EM system, *J. Appl. Geophys.*, *67*(3), 234–241, doi:10.1016/j.jappgeo.2008.05.005.

Hansen, E., S. Gerland, M. A. Granskog, O. Pavlova, A. H. H. Renner, J. Haapala, T. B. Løyning, and M. Tschudi (2013), Thinning of Arctic sea ice observed in Fram Strait: 1990–2011, *J. Geophys. Res. Oceans*, *118*, 5202–5221, doi:10.1002/jgrc.20393.

Kurtz, N., M. S. Studinger, J. Harbeck, V. Onana, and S. Farrell (2012), *IceBridge Sea Ice Freeboard, Snow Depth, and Thickness*, NASA DAAC at the Natl. Snow and Ice Data Cent., Boulder, Colo. [Updated 2013].

Kwok, R. (2009), Outflow Arctic Ocean sea ice into the Greenland and Barents Seas: 1979–2007, *J. Clim.*, *22*, 2438–2457, doi:10.1175/2008JCLI2819.1.

Kwok, R., and D. A. Rothrock (2009), Decline in Arctic sea ice thickness from submarine and ICESat records: 1958–2008, *Geophys. Res. Lett.*, *36*, L15501, doi:10.1029/2009GL039035.

Kwok, R., G. F. Cunningham, M. Wensnahan, I. Rigor, H. J. Zwally, and D. Yi (2009), Thinning and volume loss of the Arctic Ocean sea ice cover: 2003–2008, *J. Geophys. Res.*, *114*, C07005, doi:10.1029/2009JC005312.

Kwok, R., G. Spreen, and S. Pang (2013), Arctic sea ice circulation and drift speed: Decadal trends and ocean currents, *J. Geophys. Res. Oceans*, *118*, 2408–2425, doi:10.1002/jgrc.20191.

Laxon, S. W., et al. (2013), CryoSat-2 estimates of Arctic sea ice thickness and volume, *Geophys. Res. Lett.*, *40*, 732–737, doi:10.1002/grl.50193.

Maslanik, J., J. Stroeve, C. Fowler, and W. Emery (2011), Distribution and trends in Arctic sea ice age through spring 2011, *Geophys. Res. Lett.*, *38*, L13502, doi:10.1029/2011GL047735.

Nguyen, A. T., D. Menemenlis, and R. Kwok (2011), Arctic ice-ocean simulation with optimized model parameters: Approach and assessment, *J. Geophys. Res.*, *116*, C04025, doi:10.1029/2010JC006573.

Nguyen, A. T., R. Kwok, and D. Menemenlis (2012), Source and pathway of the western Arctic upper halocline in a data-constrained coupled ocean and sea ice model, *J. Phys. Oceanogr.*, *42*, 802–823, doi:10.1175/JPO-D-11-040.1.

Onogi, K., et al. (2007), The JRA-25 reanalysis, *J. Meteorol. Soc. Jpn.*, *85*, 369–432.

Parkinson, C. L., and J. C. Comiso (2013), On the 2012 record low Arctic sea ice cover: Combined impact of preconditioning and an August storm, *Geophys. Res. Lett.*, *40*, 1356–1361, doi:10.1002/grl.50349.

Perovich, D., J. Richter-Menge, C. Polashenski, B. Elder, T. Arbetter, and O. Brennick (2014), Sea ice mass balance observations from the North Pole Environmental Observatory, *Geophys. Res. Lett.*, *41*, 2019–2025, doi:10.1002/2014GL059356.

Pfirman, S., W. F. Haxby, R. Colony, and I. Rigor (2004), Variability in Arctic sea ice drift, *Geophys. Res. Lett.*, *31*, L16402, doi:10.1029/2004GL020063.

Rampal, P., J. Weiss, and D. Marsan (2009), Positive trend in the mean speed and deformation rate of Arctic sea ice, 1979–2007, *J. Geophys. Res.*, *114*, C05013, doi:10.1029/2008JC005066.

Renner, A. H. H., M. Dumont, J. Beckers, S. Gerland, and C. Haas (2013), Improved characterisation of sea ice using simultaneous aerial photography and sea ice thickness measurements, *Cold Reg. Sci. Technol.*, *92*, 37–47, doi:10.1016/j.coldregions.2013.03.009.

Richter-Menge, J. A., and S. L. Farrell (2013), Arctic sea ice conditions in spring 2009–2013 prior to melt, *Geophys. Res. Lett.*, *40*, 5888–5893, doi:10.1002/2013GL058011.

Spreen, G., S. Kern, D. Stammer, and E. Hansen (2009), Fram Strait sea ice volume export estimated between 2003 and 2008 from satellite data, *Geophys. Res. Lett.*, *36*, L19502, doi:10.1029/2009GL039591.

Spreen, G., R. Kwok, and D. Menemelis (2011), Trends in Arctic sea ice drift and role of wind forcing: 1992–2009, *Geophys. Res. Lett.*, *38*, L19501, doi:10.1029/2011GL048970.

Tome, A. R., and P. M. A. Miranda (2004), Piecewise linear fitting and trend changing points of climate parameters, *Geophys. Res. Lett.*, *32*, L02207, doi:10.1029/2003GL019100.